

DETAILED CHEMISTRY LES-CMC SIMULATIONS OF LEAN BLOW-OFF IN KEROSENE SPRAY FLAMES

J. M. Foale¹, A. Giusti², E. Mastorakos¹

¹ *Department of Engineering, University of Cambridge*

² *Department of Mechanical Engineering, Imperial College London*

jmf86@cam.ac.uk

15-17 Sept. 2021

Abstract

The objective of this work is to simulate with Large-Eddy Simulation and the Conditional Moment Closure combustion sub-grid model the lean blow-off (LBO) curve of a realistic liquid-fuelled flame. The simulation provides sufficient detail to explore the physics of LBO phenomena relating to: flame structure, intermediate species behaviour, fuel evaporation and fuel starvation. Three kerosene spray flames studied previously experimentally in the Cambridge bluff-body swirl burner are simulated and it is found that LES-CMC reproduces the experimental LBO points within 20% accuracy. The blow-off duration falls in the range 10-30 ms and asymmetric flame structures are observed before blow-off, both comparing well with experiments. CH_2O was observed to enter the recirculation zone from downstream during LBO and was present in regions of low to intermediate temperature. The temperature is observed to reduce in the recirculation zone, thus evaporation cannot keep up in the flame region. Reduced temperature is also an obstacle to the pyrolysis of the kerosene vapour, so the flame is starved of fuel, causing the stoichiometric mixture fraction isosurface to shrink down toward the bluff body until it exists only around the injected spray. Fuel starvation is a significant factor in the blow-off of spray flames.

1 Introduction

Liquid fuels and lean combustion will be necessary in the aviation industry for decades to come, thus a strong fundamental understanding of spray flames of realistic fuels at extreme conditions like lean blow-off (LBO) must be pursued by combustion scientists to improve stability and reduce emissions. Spray flames are characterised by a wide range of scales and physical processes (Jenny et al., 2012) where both flame-turbulence interaction and spray evaporation play a strong role in determining local flame structure (Olguin and Gutheil, 2014) and extinction behaviour. Recently studied experimentally at laboratory-scale with various liquid fuels (Cavaliere et al., 2013; Yuan et al., 2018; Allison et al., 2018), non-premixed and spray flames operated in the vicinity of blow-off are usu-

ally characterised by the presence of local extinctions which eventually develop into the global extinction of the flame. There is experimental evidence that spray flame blow-off has some salient differences from gaseous flame blow-off (Cavaliere et al., 2013), so a better fundamental understanding of the coupling between the multi-physical processes involved in the local and global extinction of spray flames is still necessary. A numerical approach capable of capturing the finite rate chemistry effects, with all the physical processes leading to the extinction transient included, is required to reliably predict the extinction behaviour.

This work aims to complement previous investigations of modelling LBO of kerosene spray flames (Escalpez et al., 2017) by using the Large Eddy Simulation (LES) Conditional Moment Closure (CMC) approach with a focus on fuel evaporation and LBO phenomena. The burner is the Cambridge lab-scale bluff body swirl-stabilised spray burner numerically studied previously with n-heptane (Tyliszczak et al., 2014) and ethanol (Giusti and Mastorakos, 2017). The LES-CMC approach, which has had demonstrated success capturing local and global extinction for gaseous (Zhang et al., 2015; Zhang and Mastorakos, 2016) and spray flames (Giusti and Mastorakos, 2016, 2017), is used here with Lagrangian spray modelling and a detailed Hybrid Chemistry mechanism for Jet-A (Wang et al., 2018; Xu et al., 2018). Experimental evidence of the extinction transient of heavy fuels (Pathania et al., 2020) suggests significant low- and high-temperature chemical effects during the LBO process. Hence, using a complex chemical scheme for kerosene allows exploration of the full range of behaviours to be explored by simulation. The objectives of this work are: (i) to predict lean blow-off phenomena such as local extinction and fuel starvation, (ii) to investigate the flame structure, species and the interaction between turbulence and evaporation during global lean blow-off, and (iii) to simulate the experimental blow-off curve of Jet-A spray flames.

2 Methods and configuration

The lean blow-off behaviour of kerosene spray flames is investigated using the LES-CMC ap-

proach (Klimenko and Bilger, 1999; Mortensen and Bilger, 2009). This method is based on the solution of conditionally filtered mass fraction of species and enthalpy. It allows for a direct computation of the transient of the local flame structure in mixture fraction space, and as a function of time and physical space, including turbulence effects, micro-mixing and evaporation. First order closure is used for the chemical source terms with the reaction rate evaluated using the detailed HyChem mechanism for Jet-A, consisting of 119 species and 843 reactions (Wang et al., 2018). The CMC equations were solved using an unstructured in-house code (Garmory and Mastorakos, 2015; Giusti and Mastorakos, 2016) implemented in OpenFOAM 2.3.1 using an Eulerian-Lagrangian approach for dilute sprays (Sitte and Mastorakos, 2019), the Abramzon and Sirignano (1989) evaporation model and time step of $1 \mu\text{s}$. The same computational setup used in Foale et al. (2021) for the solution of both the flow field and CMC equations was adopted in this study.

The bluff-body spray swirl burner geometry used in this study was previously explored experimentally (Yuan et al., 2018; Sidey et al., 2017; Allison et al., 2018) and numerically (Tyliszczak et al., 2014; Giusti and Mastorakos, 2017; Foale et al., 2019, 2021). The burner is enclosed in a quartz rectangular enclosure that is open at the top, exposed to atmospheric pressure. The fuel spray is injected as a hollow cone from the centre of the 25 mm bluff-body at a 60° angle with Sauter Mean Diameter of $60 \mu\text{m}$. In this study the flame is simulated at three fuel mass flow rates: 0.27 g/s , 0.30 g/s and 0.33 g/s . Air is swirled clockwise through a 60° swirler in the annular duct with outer diameter of 37 mm surrounding the bluff-body. Stable air bulk velocities from which blow-off was initiated corresponding to the respective fuel mass flow rates were: 15.9 m/s , 18.6 m/s , and 22.1 m/s . The stable 0.27 g/s case is the original, from which the fuel and air mass flow rates were increased to generate the successive 0.30 g/s case. From this case the $\dot{m}_f = 0.33 \text{ g/s}$ case was similarly generated. The simulations were run for 5 ms to stabilise before commencing blow-off. To initiate blow-off, the air mass flow rates were increased in steps by 10% until matching the blow-off air bulk velocities $U_{BO,exp}$ reported for Jet-A in Allison et al. (2018). In the $\dot{m}_f = 0.27 \text{ g/s}$ case, $U_b = 1.05U_{BO,exp}$ was high enough to bring OH mass fraction and temperature levels low enough to be considered extinguished. The 0.30 g/s and 0.33 g/s fuel mass flow rate cases required increased blow-off velocities beyond experimental values due to their rates of isosurface area, heat release and evaporation being less sensitive to the increased air than the $\dot{m}_f = 0.27 \text{ g/s}$ case. The time $t = 0 \text{ ms}$ in Section 3 figures indicates the beginning of the blow-off transient, the first instance the experimental blow-off air velocity was injected.

3 Results and discussion

After increasing the bulk air velocities to the experimental values, the simulations underwent the blow-off transient. In all cases, the air velocity was increased beyond the experimental values to ensure blow-off, to speeds 5-20% higher than those observed in experiments. Final U_b values are recorded in Table 1 and graphical comparison with the experimental blow-off curve is in Fig. 1.

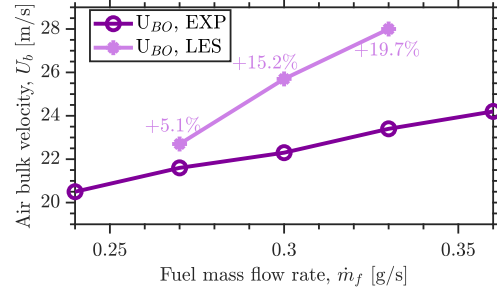


Figure 1: LBO curve comparing LES-CMC blow-off bulk air velocities with experimental values for Jet-A from Allison et al. (2018).

Table 1: Simulation fuel mass flow rates (\dot{m}_f), final blow-off bulk velocities (U_b), overall equivalence ratio ($\phi_{overall}$), and comparison with experimental blow-off velocities.

\dot{m}_f (g/s)	U_b (m/s)	$\phi_{overall}$	$U_b/U_{BO,exp}$
0.27	22.7	0.26	105%
0.30	25.7	0.25	115%
0.33	28.0	0.25	120%

The blow-off transients in the flame zone are visualised quantitatively using conditional stoichiometric temperature averaged over the stoichiometric mixture fraction isosurface area in Fig. 2 and using the volume integrated heat release (HR) from 3D cells located along the stoichiometric mixture fraction isosurface in Fig. 3. Figure 2 shows both the conditional stoichiometric isosurface-averaged temperature and

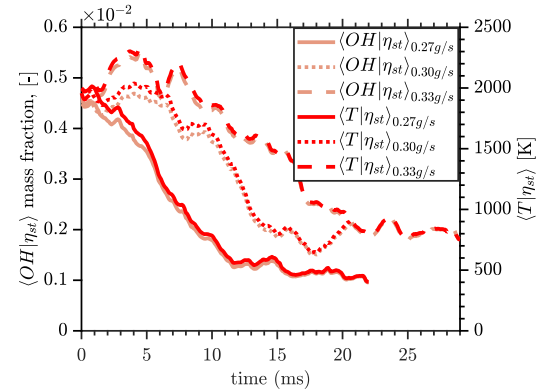


Figure 2: OH mass fraction and temperature (K) averaged over isosurface area, conditioned on stoichiometric mixture fraction ($\eta_{st} = 0.0637$) during LBO.

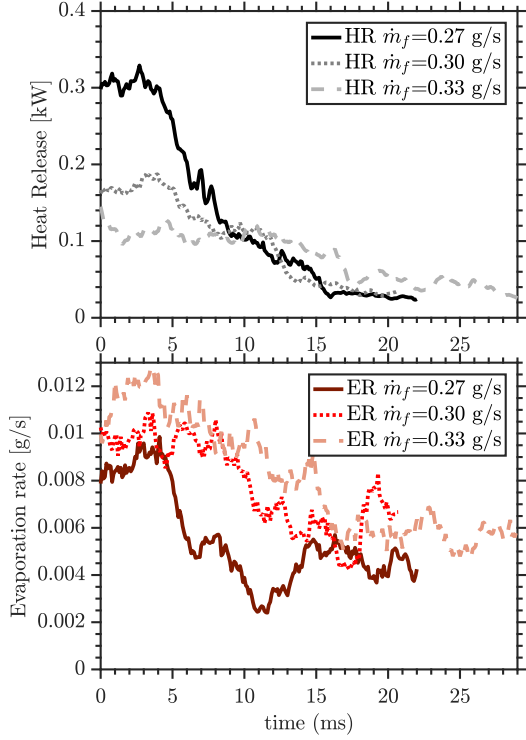


Figure 3: Heat release (top) and evaporation rate (bottom) integrated from cell volumes along the stoichiometric ($\eta_{st} = 0.0637$) isosurface.

OH mass fraction decrease fairly monotonically for the three cases, before levelling out to values indicative of an extinguished flame. The rates of decrease vary between the cases; the length of the blow-off transient appears to increase with increasing fuel mass flow rate. Using an extinction temperature threshold of 1200 K, determined using 70% of the temperature value in the 0D-CMC solution prior to extinction (see Zhang and Mastorakos (2016) or Foale et al. (2021) for details). Fig. 2 shows the flame blowoff event lasts between about 7 to 17 ms for the three mass flow rates.

Another way to estimate the blow-off transient time is through the change in heat release. Figure 3 shows the heat release and evaporation rate in the regions of stoichiometric mixture fraction for the three cases. The simulations in Fig. 3 experienced 89.5%, 80.3% and 81.2% reductions in heat release for $\dot{m}_f = 0.27$ g/s, 0.30 g/s and 0.33 g/s respectively. Using a threshold of 80% reduction in heat release to signify blow-off of the flame, the blow-off times are 14.8 ms, 17.9 ms and 28.6 ms. These blow-off transient durations all fall within the expected range compared with decane and dodecane spray flame experiment blow-off times in Yuan et al. (2018).

Reductions in the heat release in the flame stoichiometric region are linked to the evaporation rate, shown in the bottom of Fig. 3. As evaporation rate decreases over time, so does heat release. However after a certain point evaporation rate increases again, it does not necessarily mean the heat release will increase, as seen in the $\dot{m}_f = 0.27$ g/s flame. Evapora-

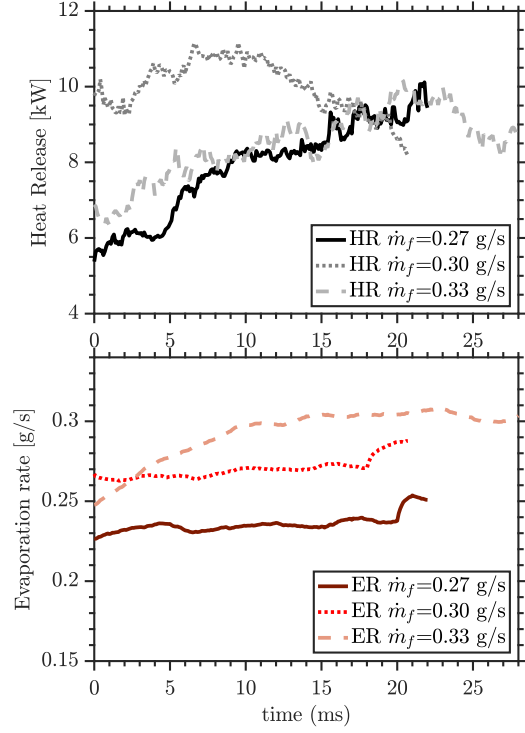


Figure 4: Heat release (top) and evaporation rate (bottom) integrated over entire chamber volume.

tion rate at stoichiometry is higher at larger fuel mass flow rates. The physical understanding for the cause of LBO in non-premixed flames is that local extinctions, or holes, in the flame surface increase in size and duration until the flame is extinguished globally. In Foale et al. (2021) local extinctions of the $\dot{m}_f = 0.27$ g/s flame were identified to increase in number during LBO, however their influence did not appear to be the sole reason for blow-off of the flame, as the flame isosurface shrank downward and inward toward the centre of the bluff body. Decreased presences of gaseous fuel and pyrolysis products were observed during blow-off. In Fig. 3 the evaporation rate in the flame zone decreases considerably, supporting the idea proposed in Cavaliere et al. (2013) that fuel starvation from reduced temperatures and evaporation is another cause for the blow-off of spray flames.

The heat release and evaporation during the blow-off transients behave quite differently taking the whole combustion chamber volume into account, as seen in Fig. 4. The mean evaporation rates in the chamber range between 87-90% of the injected fuel mass flow rates, indicating the presence of unburnt droplets in the system. Despite similar proportions of evaporated fuel in the three cases, the $\dot{m}_f = 0.30$ g/s chamber displays heat release close to the ideal heat of combustion for kerosene (≈ 11 kW) early in the blow-off transient, while the other two cases release significantly less power initially. However as time progresses, the other two cases interestingly increase in power during most of the transient, while the heat release of the $\dot{m}_f = 0.30$ g/s case decreases after about 10 ms. This in-

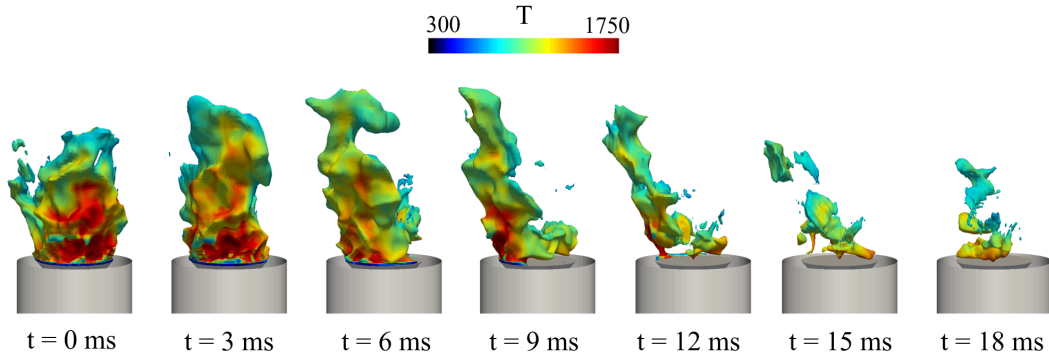


Figure 5: LBO time sequence of the 3D stoichiometric isosurface ($\eta_{st} = 0.0637$) coloured with temperature (K) for the $\dot{m}_f = 0.30$ g/s case, showing an asymmetric flame shape characteristic of low-volatility fuels close to blow-off.

creasing heat release behaviour can be attributed to increased strain rates and the presence of droplets downstream in the chamber, which continue to vaporise in the warm temperatures of the recirculation zone, producing gaseous fuel that reacts with increased quantities of fresh oxidants from the higher air mass flow rates.

Moving on to qualitative results and the structure of kerosene spray flames during LBO, Fig. 5 shows the stoichiometric mixture fraction isosurface coloured with temperature of the $\dot{m}_f = 0.30$ g/s flame during the blow-off event. The flame shape is asymmetric with a single flame branch, which rotates around the bluff body edge. This matches well with the asymmetric spray flame structures observed in Yuan et al. (2018) for decane and dodecane, where low fuel volatility was suggested to cause a lack of fuel vapour in the central recirculation zone. Significant quantities of unburnt fuel vapour (pre-pyrolysis) can also quench large regions of the flame, observed in the $\dot{m}_f = 0.27$ g/s results in Foale et al. (2021), resulting in a large local extinction which can travel with the swirling air. Once the flame is extinguished at $t = 18$ ms in Fig. 5, stoichiometric mixture fraction isosurface still persists, although only in the vicinity of the spray.

Heat release rate (HRR) during the blow-off event for the $\dot{m}_f = 0.27$ g/s case is displayed in Fig. 6. At first HRR is high along the shear layer and the flame is solidly attached to the bluff body edge. As the transient progresses the peak levels of HRR decrease and regions of very low HRR appear along both the inner and outer flame branches. These results are similar to OH-PLIF results for decane and dodecane (Yuan et al., 2018), where the inner and outer flame branches were also often disconnected and fragmented, especially near LBO.

The LBO sequence in the same 2D plane with OH mass fraction for the $\dot{m}_f = 0.33$ g/s case is shown in Fig. 7. The asymmetric flame branch is visible with medium to high values of OH as the start of LBO, but as time increases the peak OH reduces and shrinks down toward the bluff body where peaks eventually reduce to extinguished flame values. At blow-off ($t = 28$ ms), very little OH is present in the conical

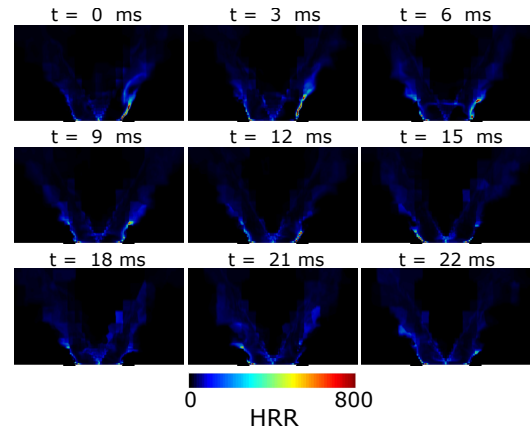


Figure 6: 2D cut-planes of the LBO sequence showing HRR (MW/m^3) for $\dot{m}_f = 0.27$ g/s flame.

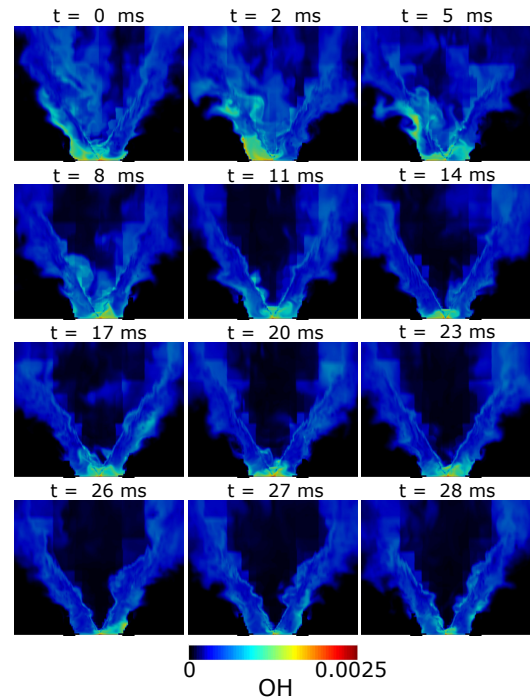


Figure 7: 2D cut-planes of the LBO time sequence showing OH mass fraction, $\dot{m}_f = 0.33$ g/s flame.

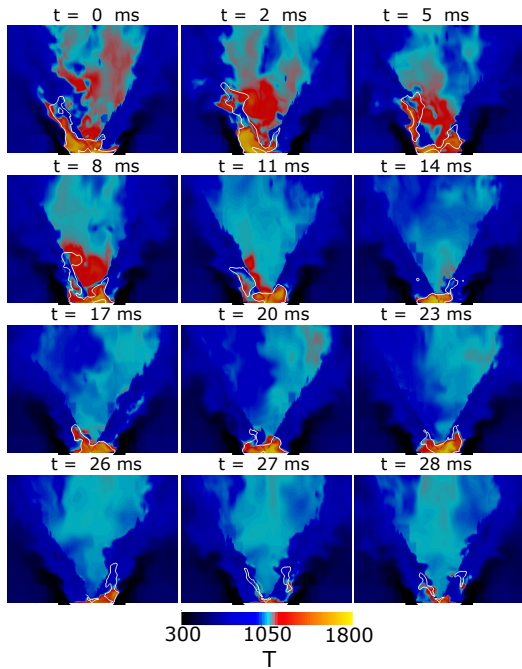


Figure 8: 2D cut-planes of the LBO time sequence of temperature (K), $\dot{m}_f = 0.33$ g/s. White iso-lines indicate stoichiometry ($\eta_{st} = 0.0637$).

central recirculation zone and none whatsoever is located around the outer corners of the chamber.

Figure 8 shows the temperature field for the same flame. The colour scale emphasises the intermediate temperature range, 1050 K being the temperature when pyrolysis of the parent fuel begins, according to shock tube experiments with Jet-A in Han et al. (2019). From time $t = 0$ ms to about 11 ms the recirculation zone contains regions hot enough to enable the full pyrolysis of the evaporated fuel, and OH is present in these corresponding regions in Fig. 7. In Fig. 8 the temperature of the recirculation zone during blow-off decreases over time due the increased amount of cold air, to the point where its temperature is at the lower threshold 1000-1050 K, below which pyrolysis of the fuel does not occur. The stoichiometric iso-lines show how the flame shrinks during the transient, after $t = 28$ ms the only location stoichiometric mixture can be observed is along the fuel spray.

CH₂O mass fraction, a marker of incomplete combustion, is shown in Fig. 9. Prior to blow-off and between $t = 0$ to 11 ms CH₂O peaks are near stoichiometry (white iso-lines) and the air shear layer. However as the blow-off transient progresses, peak CH₂O tends to appear more in regions of low to intermediate temperature, between the 500 K and 800 K temperature iso-lines, especially in regions of large gradients like the air shear layer where the iso-lines come close together. CH₂O presence gradually builds up both in the recirculation zone and the outer corners of the chamber during the blow-off transient, where temperatures are either low or decreasing from intermediate levels. This is due to the corresponding lack of OH presence in these regions, as reaction with OH is a primary CH₂O consumption pathway (Paxton et al.,

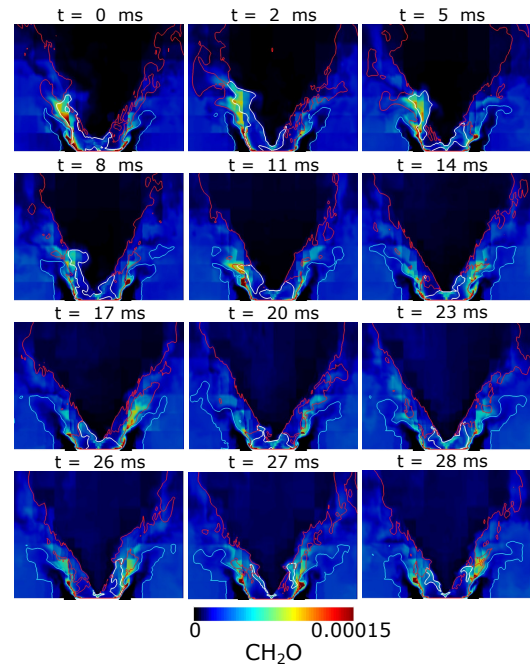


Figure 9: 2D cut-planes of the LBO time sequence of CH₂O mass fraction, $\dot{m}_f = 0.33$ g/s. White iso-line contours indicate stoichiometry ($\eta_{st} = 0.0637$), cyan lines indicate $T = 500$ K, and red lines indicate $T = 800$ K.

2019). Similar behaviour of CH₂O entering the recirculation zone from downstream during LBO was observed in pre-vapourised kerosene experiments by Pathania et al. (2020), where it was also suggested that CH₂O could act as a marker for low-temperature chemistry regions during LBO.

These LES-CMC results demonstrate the maturity of the LES-CMC turbulence-combustion model in its ability to capture finite-rate extinction and low-temperature phenomena of practical fuels.

4 Conclusions

The LES-CMC approach is used to simulate kerosene spray flames in a bluff-body swirl burner for three fuel mass flow rates at lean blow-off conditions. A high-temperature detailed mechanism developed specifically for Jet-A using the HyChem methodology is deployed. LES-CMC is able to capture asymmetric flame structural behaviour and global blow-off events at multiple fuel mass flow rates within 5-20% of experimental blow-off velocities. Heat release varied in different regions of the chamber, but was noted to decrease by at least 80% in the stoichiometric flame zone. The blow-off transient lasts between about 10-30 ms for the flames, in the same duration range as past experiments with low-volatility heavy hydrocarbon fuels. CH₂O is noted to build up in low-temperature regions between 500-800 K in the bottom corners of the chamber as well as in the recirculation zone from downstream during LBO. The effects of fuel starvation are shown to contribute to the blow-off of spray flames. Fuel starvation is caused by reduced temper-

atures in the recirculation zone, which both decreases evaporation rates as well as reduces pyrolysis of the vaporised fuel.

This work extends the LES-CMC approach capability to include modelling lean blow-off of heavy hydrocarbon liquid fuels and, by allowing the simulation of the full blow-off curve of a realistic fuel, can assist the combustion engineer in assessing operability at the design stage.

Acknowledgments

The work presented in this paper received funding from Rolls-Royce plc. The authors would like to thank the Archer UK National Supercomputing Service for use of their facilities and UKCTRF for the computational hours used in this project. We thank Prof. H. Wang for sharing the chemical mechanism used in this study.

References

- Abramzon, B. and Sirignano, W. (1989). Droplet vaporization model for spray combustion calculations. *Int. J. Heat Mass Transfer*, 32(9):1605 – 1618.
- Allison, P. M., Sidey, J. A. M., and Mastorakos, E. (2018). Lean blowoff scaling of swirling, bluff-body stabilized spray flames. *AIAA SciTech 2018*.
- Cavaliere, D. E., Kariuki, J., and Mastorakos, E. (2013). A comparison of the blow-off behaviour of swirl-stabilized premixed, non-premixed and spray flames. *Flow Turbul. Combust.*, 91(2):347–372.
- Esclapez, L., Ma, P. C., Mayhew, E., Xu, R., Stoufer, S., Lee, T., Wang, H., and Ihme, M. (2017). Fuel effects on lean blow-out in a realistic gas turbine combustor. *Combust. Flame*, 181:82–99.
- Foale, J. M., Giusti, A., and Mastorakos, E. (2019). Numerical investigation of lean blow-out of kerosene spray flames with detailed chemical models. *AIAA SciTech 2019*.
- Foale, J. M., Giusti, A., and Mastorakos, E. (2021). Simulating the blowoff transient of a swirling, bluff body-stabilized kerosene spray flame using detailed chemistry. *AIAA SciTech 2021*.
- Garmory, A. and Mastorakos, E. (2015). Numerical simulation of oxy-fuel jet flames using unstructured LES-CMC. *Proc. Combust. Inst.*, 35(2):1207 – 1214.
- Giusti, A. and Mastorakos, E. (2016). Numerical investigation into the blow-off behaviour of swirling spray flames using the LES/CMC approach. *Proc. of ETMM11, Palermo*.
- Giusti, A. and Mastorakos, E. (2017). Detailed chemistry LES/CMC simulation of a swirling ethanol spray flame approaching blow-off. *Proc. Combust. Inst.*, 36(2):2625 – 2632.
- Han, X., Liszka, M., Xu, R., Brezinsky, K., and Wang, H. (2019). A high pressure shock tube study of pyrolysis of real jet fuel Jet A. *Proc. Combust. Inst.*, 37(1):189–196.
- Jenny, P., Roekaerts, D., and Beishuizen, N. (2012). Modeling of turbulent dilute spray combustion. *Prog. Energy Combust. Sci.*, 38(6):846 – 887.
- Klimenko, A. Y. and Bilger, R. W. (1999). Conditional moment closure for turbulent combustion. *Prog. Energy Combust. Sci.*, 25(6):595 – 687.
- Mortensen, M. and Bilger, R. W. (2009). Derivation of the conditional moment closure equations for spray combustion. *Combust. Flame*, 156(1):62 – 72.
- Olguin, H. and Gutheil, E. (2014). Influence of evaporation on spray flamelet structures. *Combust. Flame*, 161(4):987 – 996.
- Pathania, R. S., Skiba, A. W., Ciardiello, R., and Mastorakos, E. (2020). Blow-off mechanisms of turbulent premixed bluff-body stabilised flames operated with vapourised kerosene fuels. *Proc. Combust. Inst.*
- Paxton, L., Giusti, A., Mastorakos, E., and Egolfopoulos, F. N. (2019). Assessment of experimental observables for local extinction through unsteady laminar flame calculations. *Combust. Flame*, 207:196–204.
- Sidey, J. A. M., Allison, P. M., and Mastorakos, E. (2017). The effect of fuel composition on swirling kerosene flames. *Proc. of 55th AIAA Aerospace Sciences Meeting*.
- Sitte, M. P. and Mastorakos, E. (2019). Large Eddy Simulation of a spray jet flame using Doubly Conditional Moment Closure. *Combust. Flame*, 199:309–323.
- Tyliszczak, A., Cavaliere, D. E., and Mastorakos, E. (2014). LES/CMC of Blow-off in a Liquid Fueled Swirl Burner. *Flow Turbul. Combust.*, 92(1-2):237–267.
- Wang, H., Xu, R., Wang, K., Bowman, C. T., Hanson, R. K., Davidson, D. F., Brezinsky, K., and Egolfopoulos, F. N. (2018). A physics-based approach to modeling real-fuel combustion chemistry - I. Evidence from experiments, and thermodynamic, chemical kinetic and statistical considerations. *Combust. Flame*, 193:502–519.
- Xu, R., Wang, K., Banerjee, S., Shao, J., Parise, T., Zhu, Y., Wang, S., Movaghar, A., Lee, D. J., Zhao, R., Han, X., Gao, Y., Lu, T., Brezinsky, K., Egolfopoulos, F. N., Davidson, D. F., Hanson, R. K., Bowman, C. T., and Wang, H. (2018). A physics-based approach to modeling real-fuel combustion chemistry - II. Reaction kinetic models of jet and rocket fuels. *Combust. Flame*, 193:520–537.
- Yuan, R., Kariuki, J., and Mastorakos, E. (2018). Measurements in swirling spray flames at blow-off. *International Journal of Spray and Combustion Dynamics*, 10(3):185–210.
- Zhang, H., Garmory, A., Cavaliere, D. E., and Mastorakos, E. (2015). Large Eddy Simulation/Conditional Moment Closure modeling of swirl-stabilized non-premixed flames with local extinction. *Proc. Combust. Inst.*, 35(2):1167 – 1174.
- Zhang, H. and Mastorakos, E. (2016). Prediction of the global extinction conditions and dynamics in swirling non-premixed flames using LES/CMC modelling. *Flow Turbul. Combust.*, 96(4):863 – 889.